

# Lowest Excited Singlet State of C<sub>60</sub>: A Vibronic Analysis of the Fluorescence

D. J. van den Heuvel, G. J. B. van den Berg, E. J. J. Groenen,\* and J. Schmidt

Centre for the Study of Excited States of Molecules, Huygens Laboratory, University of Leiden, P.O. Box 9504, 2300 RA Leiden, The Netherlands

I. Holleman and G. Meijer

Department of Molecular and Laser Physics, University of Nijmegen, Toernooiveld, 6525 ED Nijmegen, The Netherlands

Received: March 7, 1995<sup>⊗</sup>

The fluorescence and fluorescence-excitation spectra of C<sub>60</sub> in a hydrocarbon glass at 1.2 K are reported. The fluorescence spectrum resembles that of a molecular X-trap in crystalline C<sub>60</sub>. The vibronic bands in these spectra are assigned, and the intensity distribution among the false origins points to vibronic coupling within the singlet manifold. The lowest excited singlet state of C<sub>60</sub> shows predominantly T<sub>1g</sub> and G<sub>g</sub> character. Additionally, we show that a reduction of the symmetry of C<sub>60</sub> by either an intra- or an intermolecular perturbation leads to a fluorescence spectrum with a strong 0–0 transition and a different vibronic structure.

## Introduction

The degeneracy of the highest occupied and lowest unoccupied molecular orbitals of C<sub>60</sub> results in a set of close-lying low-energy excited states which, according to the common parity of these molecular orbitals, are of gerade symmetry.<sup>1</sup> Electronic transitions between these states and the ground state are symmetry forbidden. Quantum-chemical calculations indicate, in accordance with absorption data, that strong electric-dipole-allowed transitions to T<sub>1u</sub> states show up only in the ultraviolet.<sup>2</sup> Nevertheless, solutions of C<sub>60</sub> are magenta, and the solid material is black. A continuous though weak absorption of light extends all over the visible range of the electromagnetic spectrum. The present paper concerns the nature of the lowest excited states of molecular C<sub>60</sub> which are responsible for this absorption.

According to semiempirical calculations including configuration interaction, three singlet states of T<sub>2g</sub>, T<sub>1g</sub>, and G<sub>g</sub> symmetry are to be expected within 0.1 eV, i.e., so close that these calculations do not allow a conclusion regarding their order.<sup>2</sup> In addition, being orbitally degenerate and very close in energy, these states may well be subject to (pseudo) Jahn–Teller instabilities. Gasyna et al.<sup>3</sup> were among the first to study the low-lying excited states of C<sub>60</sub>. They reported absorption and magnetic-circular-dichroism spectra of C<sub>60</sub> in an argon matrix at ≈5 K and concluded on the basis of the latter spectrum that the lowest excited singlet state of C<sub>60</sub> belongs to the T<sub>1g</sub> representation. In the absorption spectrum four bands were recognized around 600 nm, which are interpreted as two Herzberg–Teller-induced false origins of the 1<sup>1</sup>T<sub>1g</sub> ← 1<sup>1</sup>A<sub>g</sub> transition, each accompanied by a band including one quantum of a Jahn–Teller active mode. Absorption spectra of C<sub>60</sub> in the visible in solution at room temperature and 77 K have been reported by Leach et al.<sup>4</sup> They assign the absorption between 410 and 620 nm to vibronic transitions that are described as Herzberg–Teller-induced false origins and superimposed, totally symmetric, and Jahn–Teller active vibrations. The observed band at 620.2 nm in *n*-hexane (γ<sub>0</sub> in their nomenclature) is considered to represent the lowest energy singlet ← singlet transition and following ref 3 is assigned as a 1<sup>1</sup>T<sub>1g</sub> ← 1<sup>1</sup>A<sub>g</sub> false origin. Their description is necessarily limited in detail because

of the fact that room-temperature and 77 K solution spectra consist of strongly overlapping, inhomogeneously broadened bands.

To unravel the nature of the low-energy excitations, a vibrationally resolved gas phase spectrum of C<sub>60</sub> would be most helpful. As yet, data are available in the 595–635 nm range from experiments on C<sub>60</sub> molecules cooled in a supersonic molecular beam.<sup>5</sup> At least seven narrow features can be distinguished. The authors consider these bands to be vibronically induced but present no further interpretation.

In view of the congestion in the low-energy part of the absorption spectrum, an easier approach to investigate the lowest singlet and triplet states is offered by luminescence and luminescence-excitation studies. The room-temperature fluorescence spectrum of C<sub>60</sub> in solution is broad and structureless. A much improved resolution has been obtained for C<sub>60</sub> in a hydrocarbon glass at 77 K.<sup>6,7</sup> This fluorescence spectrum shows a weak origin, at 655 nm in methylcyclohexane, while most of the intensity shows up in vibronic bands between 700 and 2000 cm<sup>-1</sup> from the origin. Negri et al.<sup>2</sup> presented an interpretation of this intensity distribution based on CNDO/S calculations. They take the Herzberg–Teller approach and calculate for the three lowest excited singlet states the intensity borrowed from the allowed 1<sup>1</sup>T<sub>1u</sub> ← 1<sup>1</sup>A<sub>g</sub> transitions. Comparison of their theoretical results with the fluorescence spectrum of ref 6 led them to conclude that the 1<sup>1</sup>T<sub>1g</sub> state is the lowest excited singlet state S<sub>1</sub> for C<sub>60</sub> in a hydrocarbon glass. In addition, they located the origin in absorption at 15 486 cm<sup>-1</sup> in *n*-hexane, i.e. at 646 nm and 63 cm<sup>-1</sup> higher in energy than a very weak absorption band designated β<sub>2</sub> by Leach et al.<sup>4</sup> and attributed to a triplet ← singlet transition by the latter authors.

Recently, we have reported on the fluorescence of single crystals of C<sub>60</sub> at 1.2 K.<sup>8</sup> Part of this fluorescence was interpreted as molecular C<sub>60</sub> emission from a shallow X-trap in the crystal (although we could not exclude that it derives from band-edge states). The corresponding spectrum with its origin at 684 nm (reproduced in Figure 3) is well-resolved up to 3400 cm<sup>-1</sup> from the origin. Here we present the fluorescence spectrum of C<sub>60</sub> dissolved in a decaline/cyclohexane glass at 1.2 K, which shows a much improved resolution compared to literature data from glasses at 77 K. Starting from the crystal

<sup>⊗</sup> Abstract published in *Advance ACS Abstracts*, July 1, 1995.

data, we interpret the vibronic structure of both spectra and discuss the electronic character of the lowest singlet excited state of C<sub>60</sub>. It is found that the lowest excited state of C<sub>60</sub> contains both T<sub>1g</sub> and G<sub>g</sub> character and possibly T<sub>2g</sub> character as well. This result allows us to (re)interpret part of the absorption spectra of Gasyňa et al.,<sup>3</sup> Leach et al.,<sup>4</sup> and Haufler et al.<sup>5</sup> Additionally, we show that a reduction of the symmetry of C<sub>60</sub> by either an intra- or an intermolecular perturbation leads to a fluorescence spectrum with a strong 0–0 transition and a vibronic structure different from that of C<sub>60</sub> in a hydrocarbon glass.

### Experimental Section

A solution of C<sub>60</sub> has been prepared by dissolving some C<sub>60</sub> single crystals in decaline/cyclohexane (3:1 v/v). These crystals of C<sub>60</sub> have been grown under vacuum by multiple vapor phase sublimation starting from 99.9% pure material.

To measure fluorescence and fluorescence-excitation spectra, C<sub>60</sub> was excited by an Ar<sup>+</sup> laser or an Ar<sup>+</sup> pumped dye laser. Plasma lines from the Ar<sup>+</sup> laser were suppressed using a 545 nm low pass filter. The laser powers used in this study were always so low that the emission intensity varied linearly with the excitation intensity. The emission of the sample was focused onto the entrance slit of a 1 m monochromator (resolution 0.2 nm), and fluorescence spectra were detected using an optical multichannel analyzer (EG&G OMA-Vision-CCD). We corrected these spectra for the wavelength dependence of the quantum efficiency of the CCD. For the glass and solution samples we also subtracted a monotonically decaying background signal. To obtain the fluorescence-excitation spectrum, we detected the fluorescence using a photomultiplier while scanning the excitation laser. Two detection wavelengths were used, 727 and 741 nm, and identical spectra were obtained apart from a strong Raman line of the solvent. We combined the spectra in such a way as to get rid of the Raman line. The excitation spectrum was corrected for the variation in the output intensity of the dye laser with wavelength. To perform a scan from 565 to 665 nm, we used two dyes. Wavelength calibration was performed using a neon lamp. The overall accuracy amounts to  $\pm 3$  cm<sup>-1</sup> for the fluorescence spectra and  $\pm 7$  cm<sup>-1</sup> for the fluorescence-excitation spectrum.

### Results and Interpretation

The fluorescence of C<sub>60</sub> dissolved in decaline/cyclohexane (3:1 v/v) extends from about 650 to 900 nm. While the spectrum at room temperature is not very informative, a rich vibronic structure shows up upon temperature lowering. This is illustrated in Figure 1a–c, where we present the spectrum at room temperature, at 77 K, and at 1.2 K. For the 77 K spectrum the overlap is still large and maxima are distinguishable at 656.5, 675.6, 686.7, 700.4, 713.7, 726.1, and 740.4 (precision 0.5 nm) and broader shoulders around 761 and 811 nm. At 1.2 K the width of the vibronic bands has decreased further, and a well-resolved spectrum results. We will henceforth refer to the spectrum in Figure 1c as the 658-spectrum, after the wavelength of its origin. This origin is weak, and most of the intensity in the spectrum is concentrated in bands between 720 and 760 nm. The positions and relative intensities of all vibronic bands in the 658-spectrum are summarized in Table 1. The long-wavelength region of the corresponding fluorescence-excitation spectrum at 1.2 K is shown in Figure 2, and the data on the vibronic bands are summarized in Table 2. An even better resolved fluorescence spectrum of C<sub>60</sub> has been obtained from a molecular trap in a single crystal of C<sub>60</sub> at 1.2 K.<sup>8</sup> This so-called 684-spectrum is reproduced in Figure 3. About 60

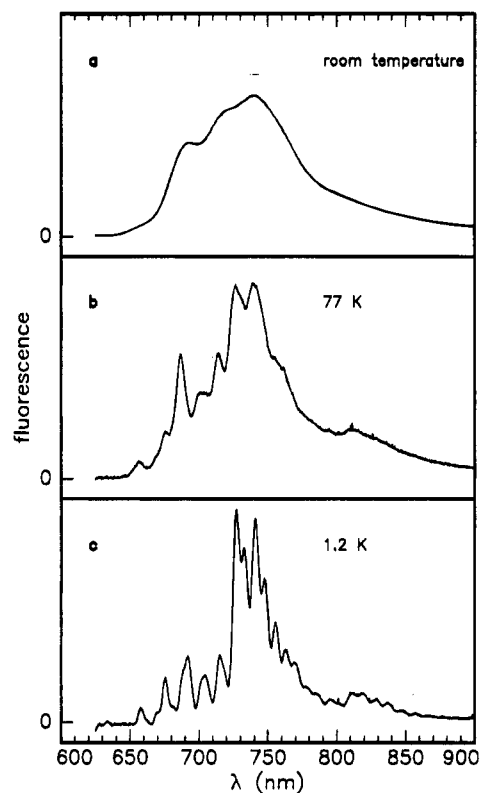


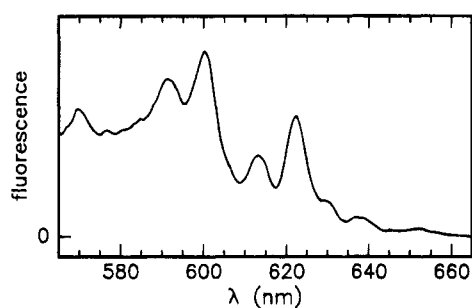
Figure 1. Fluorescence spectra of C<sub>60</sub> in decaline/cyclohexane (3:1 v/v, 5.10<sup>-4</sup> M) upon excitation at 514 nm (a) at room temperature, (b) at 77 K, and (c) at 1.2 K.

TABLE 1: Data Corresponding to the Fluorescence 658-Spectrum of C<sub>60</sub> in Decaline/Cyclohexane at 1.2 K (fig. 1c): Wavelengths, Wavenumbers, Relative Intensities, Shifts with Respect to the Origin, and Assignment of the Observed Bands (sh.: Shoulder)

λ (nm)	σ (cm <sup>-1</sup> )	int. (arb. units)	Δσ (cm <sup>-1</sup> )	assignment <sup>a</sup>
657.9	15 200	8		0–0
669.4	14 939	sh. 5	261	h <sub>g</sub> (1)
675.5	14 804	23	396	g <sub>u</sub> (1)
681.3	14 678	sh. 5	522	h <sub>u</sub> (2)
688.3	14 529	sh. 18	671	t <sub>2u</sub> (2)
692.0	14 451	33	749	h <sub>u</sub> (3)
702.4	14 237	sh. 15	963	g <sub>u</sub> (4)
704.5	14 194	22	1006	h <sub>u</sub> (3) + h <sub>g</sub> (1)
715.4	13 978	32	1222	t <sub>2u</sub> (4)
727.0	13 755	100	1445	t <sub>1u</sub> (4)
733.3	13 637	60	1563	h <sub>u</sub> (7)
741.1	13 493	95	1707	t <sub>1u</sub> (4) + h <sub>g</sub> (1)
747.8	13 373	45	1827	h <sub>u</sub> (7) + h <sub>g</sub> (1)
755.6	13 235	48	1965	t <sub>1u</sub> (4) + 2h <sub>g</sub> (1)
763.0	13 106	35	2094	h <sub>u</sub> (7) + 2h <sub>g</sub> (1)
769.7	12 992	25	2208	t <sub>1u</sub> (4) + 3h <sub>g</sub> (1)
778.2	12 850	14	2350	h <sub>u</sub> (7) + 3h <sub>g</sub> (1)
785.6	12 729	12	2471	t <sub>1u</sub> (4) + 4h <sub>g</sub> (1)
796.0	12 563	10	2637	h <sub>u</sub> (7) + 4h <sub>g</sub> (1)
811.1	12 329	13	2871	t <sub>1u</sub> (4) + h <sub>g</sub> (7)
818.5	12 217	12	2983	h <sub>u</sub> (7) + h <sub>g</sub> (7)
828.8	12 066	9	3134	t <sub>1u</sub> (4) + h <sub>g</sub> (7) + h <sub>g</sub> (1)
837.3	11 943	7	3257	h <sub>u</sub> (7) + h <sub>g</sub> (7) + h <sub>g</sub> (1)
847.8	11 795	4	3405	t <sub>1u</sub> (4) + h <sub>g</sub> (7) + 2h <sub>g</sub> (1)
857.4	11 663	2	3537	h <sub>u</sub> (7) + h <sub>g</sub> (7) + 2h <sub>g</sub> (1)
866.3	11 543	1	3657	t <sub>1u</sub> (4) + h <sub>g</sub> (7) + 3h <sub>g</sub> (1)

<sup>a</sup> The vibrational modes are labeled according to the irreducible representation they belong to. The modes within each representation are numbered starting from the lowest frequency mode.

vibronic bands may be clearly recognized up to 3400 cm<sup>-1</sup> from the weak origin at 683.6 nm with an average bandwidth of only 30 cm<sup>-1</sup>. The intensity is maximum for a band at 757.3 nm,



**Figure 2.** Fluorescence-excitation spectrum of  $C_{60}$  in decaline/cyclohexane (3:1 v/v) at 1.2 K ( $5.10^{-4}$  M).

**TABLE 2: Data Corresponding to the Fluorescence-Excitation Spectrum of  $C_{60}$  in Decaline/Cyclohexane at 1.2 K (fig. 2): Wavelengths, Wavenumbers, Relative Intensities, Shifts with Respect to the Origin, and Assignment of the Observed Bands (sh.: Shoulder)<sup>a</sup>**

$\lambda$ (nm)	$\sigma$ ( $\text{cm}^{-1}$ )	int. (arb. units)	$\Delta\sigma$ ( $\text{cm}^{-1}$ )	assignment	band code
652.2	15 333	4		0-0	$\sim\beta_2$
640.4	15 615	sh. 4	282	$h_g(1)$	
636.8	15 704	10	371	$h_u(1)/g_u(1)$	
630.1	15 870	sh. 13	537	$h_u(2)$	$\beta_3$
622.3	16 069	65	736	$h_u(3)$	$\gamma_0$
613.7	16 295	sh. 30	962	$g_u(4)$	} $\gamma_1$
612.5	16 327	40	994	$h_u(3) + h_g(1)$	
600.3	16 658	100	1325	$t_{1u}(4)$	$\gamma_2$
592.0	16 892	70	1559	$h_u(7)$	} $\gamma_3$
591.0	16 920	80	1587	$t_{1u}(4) + h_g(1)$	
576.7	17 340	20	2007		
569.9	17 547	60	2214		$\gamma_5$

<sup>a</sup> The band codes in the last column are the labels of the corresponding bands in the absorption spectrum of  $C_{60}$  in *n*-hexane at room temperature introduced by Leach et al.<sup>4</sup>

1425  $\text{cm}^{-1}$  from the origin. A survey of most of the vibronic bands below 2200  $\text{cm}^{-1}$  from the origin is given in Table 3 (only those bands with an intensity at least about 10% of that of the 1425  $\text{cm}^{-1}$  band have been included).

To interpret the vibronic structure of the fluorescence, we make use of literature data on vibrational frequencies and predicted intensities of false origins. For the infrared ( $t_{1u}$ ) and Raman ( $a_g$ ,  $h_g$ ) active modes we base our interpretations on experimental frequencies observed for  $C_{60}$  films.<sup>9</sup> For the other modes we take the vibrational frequencies calculated by Jishi et al.,<sup>10</sup> who optimized their force-constant model in order to simulate the frequencies of the Raman active modes. The oscillator strengths of the vibronically induced transitions between the  $^1A_g$  ground state and the close-lying  $^1T_{2g}$ ,  $^1T_{1g}$ , and  $^1G_g$  states have been calculated by Negri et al.<sup>2</sup> using the CNDO/S method. The literature data regarding normal mode frequencies and vibronic intensities that form the basis for our description of the fluorescence spectra are summarized in Table 4.

First we consider the spectrum richest in vibronic structure, the 684-spectrum in Figure 3, Table 3. The origin is weak, which is consistent with the electric-dipole-forbidden character of the transition between the lowest excited singlet state, whether  $T_{1g}$ ,  $T_{2g}$ , or  $G_g$  in nature, and the ground state. Although weak, the origin is observable, which most probably reflects the reduced symmetry of the crystal field at the distorted trap site. (The site symmetry in the simple-cubic  $C_{60}$  lattice is  $S_6$ , which would maintain the parity-forbidden character of the origin.) The most intense vibronic band is found at 1425  $\text{cm}^{-1}$  from the origin. Comparison with Table 4 shows that this band probably corresponds to the transition from the vibrationless excited state to the electronic ground state including one

**TABLE 3: Data Corresponding to the 684-Spectrum of Crystalline  $C_{60}$  at 1.2 K (fig. 3): Wavelengths, Wavenumbers, Relative Intensities, Shifts with Respect to the Origin, and Assignment of the Observed Bands (sh.: Shoulder)<sup>a</sup>**

$\lambda$ (nm)	$\sigma$ ( $\text{cm}^{-1}$ )	int. (arb. units)	$\Delta\sigma$ ( $\text{cm}^{-1}$ )	assignment
683.6	14 629	18		0-0
684.9	14 601	sh. 10	28	<i>s</i>
695.9	14 370	10	259	$h_g(1)$
700.0	14 286	9	343	$h_u(1)$
702.5	14 235	11	394	$g_u(1)$
709.1	14 102	21	527	$h_u(2)$
715.9	13 968	19	661	$t_{2u}(2)$
719.6	13 897	55	732	$h_u(3)$
721.3	13 868	20	761	$g_u(2)/h_u(3)$ ( <i>s</i> )
731.4	13 673	28	956	$g_u(4)$
733.7	13 629	28	1000	$h_u(3) + h_g(1)$
735.3	13 600	sh. 10	1029	$h_u(3) + h_g(1)$ ( <i>s</i> )
743.4	13 452	sh. 10	1177	$t_{1u}(3)$
745.2	13 419	38	1210	$t_{2u}(4)$
750.6	13 323	53	1306	$g_u(5)$
752.0	13 298	sh. 20	1331	$g_u(5)$ ( <i>s</i> )
757.3	13 204	100	1425	$t_{1u}(4)$
760.1	13 157	sh. 33	1472	$t_{1u}(4)$ ( <i>s</i> )
765.3	13 067	36	1562	$h_u(7)$
767.6	13 028	sh. 20	1601	$h_u(7)$ ( <i>s</i> )
773.0	12 937	28	1692	$t_{1u}(4) + h_g(1)$
775.6	12 893	sh. 15	1736	$t_{1u}(4) + h_g(1)$ ( <i>s</i> )
781.1	12 802	21	1827	$h_u(7) + h_g(1)$
782.7	12 776	sh. 10	1853	$h_u(7) + h_g(1)$ ( <i>s</i> )
786.3	12 718	9	1911	
789.0	12 674	12	1955	$t_{1u}(4) + 2h_g(1)$
792.3	12 621	10	2008	
797.5	12 539	9	2090	$h_u(7) + 2h_g(1)$
800.1	12 499	12	2130	
804.4	12 433	11	2196	

<sup>a</sup> The bands marked *s* belong to a minority of  $C_{60}$  molecules in a different crystal site. These mostly appear as shoulders at the long-wavelength side of intense bands, shifted by  $35 \pm 10$   $\text{cm}^{-1}$ . Only bands with a relative intensity up to about 10% have been included.

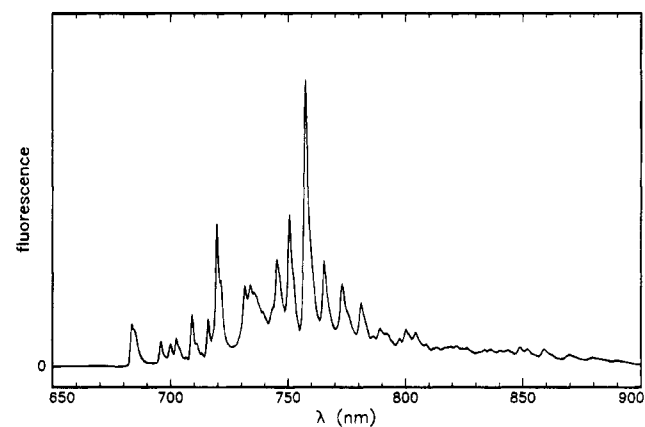


**Figure 3.** Fluorescence spectrum of a shallow molecular  $C_{60}$  trap in crystalline  $C_{60}$  at 1.2 K upon excitation at 514 nm.

quantum of the  $t_{1u}(4)$  vibrational mode. According to the calculations of Negri et al., this conclusion would point to a  $T_{1g}$  character of the lowest excited singlet state  $S_1$ . These calculations predict that for such an assignment the intensity should be concentrated in two false origins, those based on the  $t_{1u}(4)$  and  $h_u(7)$  modes, with relative intensities about 4 to 1. Significant intensity is indeed present in the 684-spectrum at 1562  $\text{cm}^{-1}$  from the origin, corresponding to the  $h_u(7)$  band. However, substantial intensity is also found for bands at 394, 527, 661, 732, 761, 1210, and 1306  $\text{cm}^{-1}$  from the origin, bands that can be assigned to  $g_u(1)$ ,  $h_u(2)$ ,  $t_{2u}(2)$ ,  $h_u(3)$ ,  $g_u(2)$ ,  $t_{2u}(4)$ , and  $g_u(5)$  modes, respectively. Such a vibronic intensity

**TABLE 4: Summary of the Frequencies of the Herzberg–Teller Active Vibrations for the Three Lowest Excited Singlet States and the Calculated Oscillator Strengths of the Possible False Origins<sup>a</sup>**

T <sub>1g</sub>		T <sub>2g</sub>		G <sub>g</sub>	
mode	<i>f</i> × 10 <sup>4</sup>	mode	<i>f</i> × 10 <sup>4</sup>	mode	<i>f</i> × 10 <sup>4</sup>
a <sub>u</sub> 1142	0	g <sub>u</sub> 385	6	t <sub>2u</sub> 367	0
		789	1	677	8
t <sub>1u</sub> 527	0	929	2	1025	0
577	0	961	16	1212	3
1183	6	1327	0	1575	0
1428	75	1413	72		
				g <sub>u</sub> 385	6
h <sub>u</sub> 361	5	h <sub>u</sub> 361	26	789	33
543	0	543	0	929	3
700	3	700	0	961	0
801	0	801	1	1327	24
1129	6	1129	2	1413	0
1385	0	1385	0		
1552	19	1552	85	h <sub>u</sub> 361	0
				543	21
				700	93
				801	9
				1129	0
				1385	2
				1552	2

<sup>a</sup> The vibrational frequencies of the t<sub>1u</sub> modes are experimental values;<sup>9</sup> those of the other modes concern values calculated by Jishi et al.<sup>10</sup> The oscillator strengths represent values calculated by Negri et al.<sup>2</sup> Note that the frequencies of the normal modes came out slightly different in their calculations.

distribution is unexpected for a T<sub>1g</sub> assignment of S<sub>1</sub> and, according to the CNDO/S calculations, would be compatible with an assignment of S<sub>1</sub> as G<sub>g</sub>. The occurrence of bands at 343 and 956 cm<sup>-1</sup> might hint toward a minor T<sub>2g</sub> character of S<sub>1</sub>. On the other hand, the intensity of the h<sub>u</sub>(7) mode is qualitatively in agreement with that expected on the basis of a T<sub>1g</sub> assignment, and the T<sub>2g</sub> active g<sub>u</sub>(6) mode seems to be absent (unless its actual frequency is somewhat higher such that this mode coincides with the t<sub>1u</sub>(4) mode). Whether or not S<sub>1</sub> has T<sub>2g</sub> character as well can only be judged after a more elaborate theoretical treatment. As yet, we conclude from the vibronic intensity distribution of the fluorescence that for the shallow molecular trap in the single crystal of C<sub>60</sub> the S<sub>1</sub> state at 14 629 cm<sup>-1</sup> has predominantly mixed T<sub>1g</sub>, G<sub>g</sub> character. This may be rationalized in terms of an appreciable vibronic (pseudo-Jahn–Teller) interaction between the 1<sup>1</sup>T<sub>1g</sub> and 1<sup>1</sup>G<sub>g</sub> excited states, which in I<sub>h</sub> symmetry have been calculated very close in energy. The 684-spectrum further shows evidence for a Jahn–Teller distortion of C<sub>60</sub> in S<sub>1</sub>. The active h<sub>g</sub>(1) mode may be recognized 259 cm<sup>-1</sup> from the origin and in combination bands with h<sub>u</sub>(3), t<sub>1u</sub>(4), and h<sub>u</sub>(7). Finally, we note that additional weaker bands are present in the spectrum shifted by 35 ± 10 cm<sup>-1</sup> with respect to main bands (since they appear as shoulders, it is difficult to determine their positions). We attribute these to a C<sub>60</sub> molecule in a slightly different crystal site, and therefore label these *s*. The shoulder of the t<sub>1u</sub>(4) band may contain a contribution of the a<sub>g</sub>(2) band as well. The complete assignment of the fluorescence spectrum in Figure 3 is given in the last column of Table 3.

With the analysis of the 684-spectrum as a starting point it is only a small step to the interpretation of the fluorescence spectrum of C<sub>60</sub> in decaline/cyclohexane at 1.2 K. The origin at 657.9 nm is again weak. It is shifted by 571 cm<sup>-1</sup> to the blue compared with that for C<sub>60</sub> in the crystalline environment where the dispersion interaction is stronger. The vibronic bands in the 658-spectrum are broader than in the 684-spectrum, owing to the larger inhomogeneity of the molecular surroundings in

the glass. Consequently, less of the weaker vibronic bands are resolved, but most features of the spectrum discussed above show up in the glass spectrum as well, albeit with a somewhat different intensity distribution. The central part of the spectrum reveals four intense bands, two fundamental and two combination bands. The prominence of the t<sub>1u</sub>(4) and h<sub>u</sub>(7) modes again refers to the T<sub>1g</sub> character of S<sub>1</sub>, while the occurrence of modes of lower frequencies indicates G<sub>g</sub> character as well. The amount of G<sub>g</sub> character seems to be less for C<sub>60</sub> in the glass, since the h<sub>u</sub>(2), h<sub>u</sub>(3), g<sub>u</sub>(2), and g<sub>u</sub>(5) modes have weaker intensity in the 658-spectrum than in the 684-spectrum. The shift of the t<sub>1u</sub>(4) mode from 1425 cm<sup>-1</sup> in the crystal to 1445 cm<sup>-1</sup> in the glass is remarkable. This infrared active mode might be more sensitive to the intermolecular interactions, owing to the fact that this vibration induces an electric dipole moment. Moreover, it is the one strongly involved in vibronic coupling. Progressions in the h<sub>g</sub>(1) mode, in particular superimposed on one quantum of the t<sub>1u</sub>(4) or h<sub>u</sub>(7) modes, are more intense and consequently longer in the glass than in the crystal and actually dominate the spectrum above 1600 cm<sup>-1</sup> from the origin. In addition, from 2871 cm<sup>-1</sup> onward progressions in h<sub>g</sub>(1) based on t<sub>1u</sub>(4) + h<sub>g</sub>(7) and h<sub>u</sub>(7) + h<sub>g</sub>(7) combinations may be recognized. The observation of bands involving h<sub>g</sub> modes clearly indicates a distortion of C<sub>60</sub> in S<sub>1</sub> along these Jahn–Teller active coordinates.

The origin of the fluorescence-excitation spectrum of C<sub>60</sub> in decaline/cyclohexane at 1.2 K is found at 652.2 nm. The Stokes shift amounts to about 130 cm<sup>-1</sup>, which corresponds to the difference between S<sub>0</sub> and S<sub>1</sub> in the dispersion interaction of C<sub>60</sub> with the environment. The frequencies of most of the vibronic bands in this spectrum up to 1600 cm<sup>-1</sup> from the origin allude to a mirror-image relation between fluorescence and excitation spectrum: 282 (261), 371 (396), 537 (522), 736 (749), 962 (963), 994 (1006), and 1559 (1563) cm<sup>-1</sup>, where the wavenumbers in parentheses refer to the vibronic bands in the fluorescence spectrum. The differences are not significant given the uncertainty in the values from the excitation spectrum, owing to the width of the vibronic bands in this spectrum. This broadening relative to the fluorescence spectrum also precludes the observation of bands in the excitation spectrum corresponding to the bands at 671 and 1222 cm<sup>-1</sup> in the fluorescence spectrum. While the frequencies do correspond largely, the intensity distribution shows differences. Particularly significant seems the greater intensity of the h<sub>u</sub>(3) mode, which may well point to an increased G<sub>g</sub> character of the Franck–Condon excited state compared with that of the relaxed fluorescent state. The one and most intriguing exception to the mirror-image relation concerns the vibronic band of maximum intensity at 1325 cm<sup>-1</sup> from the origin in the fluorescence-excitation spectrum and at 1445 cm<sup>-1</sup> in the fluorescence spectrum. We may interpret this band as corresponding to the transition from the vibrationless ground state to the first excited singlet state including one quantum of the t<sub>1u</sub>(4) vibration, and we consider the vibronic coupling between singlet excited states to be responsible for the softening of the t<sub>1u</sub>(4) mode.

The fluorescence-excitation spectrum is clearly less resolved than the fluorescence spectrum. The apparent broadening of the vibronic bands may point to the presence of additional bands, weaker and not leading to distinct maxima, corresponding to transitions into singlet states above the lowest energy S<sub>1</sub> level. Unfortunately, the excitation spectrum does not reveal an additional origin, which is understandable in view of the expected weakness of such a transition. However, the continuous and high intensity above 1600 cm<sup>-1</sup> from the origin does not have a counterpart in the fluorescence spectrum, and in

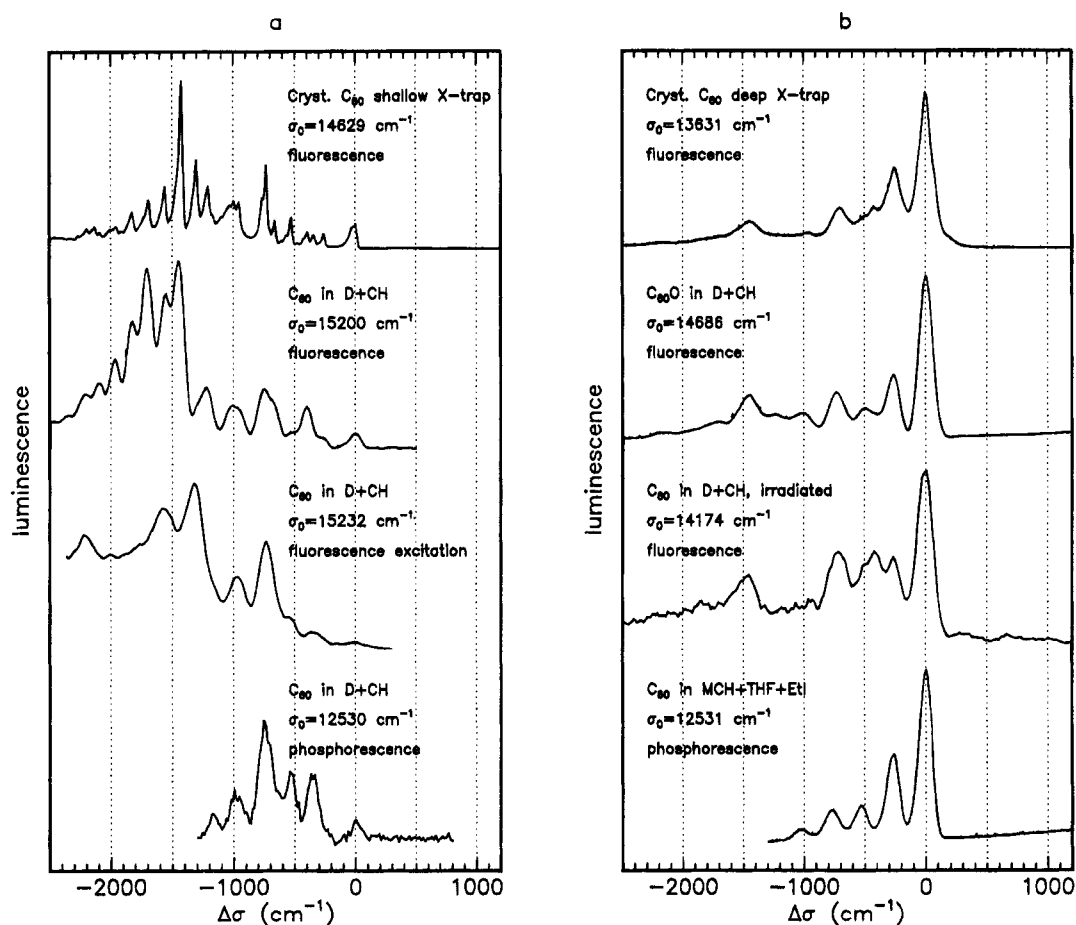


**Figure 4.** Fluorescence, fluorescence-excitation, and phosphorescence spectra of  $C_{60}$  and some  $C_{60}$ -related species at 1.2 K: (a) those with a weak origin; (b) those with a strong origin. The spectra have been shifted with respect to each other, and the horizontal axes represent wavenumber scales relative to their origins. The values of  $\sigma_0$  denote the actual wavenumbers of the electronic origins. The fluorescence-excitation spectrum has been inverted with respect to the origin to allow comparison of the vibronic structure with that of the emission spectra. (D = decaline, CH = cyclohexane, MCH = methylcyclohexane, THF = tetrahydrofuran, EtI = ethyl iodide.)

particular, the maxima distinguishable at 2007 and 2214  $\text{cm}^{-1}$  may well concern false origins of the  $S_2 \leftarrow S_0$  transition.

From Figure 1 it is clear that the fluorescence becomes less resolved with increasing temperature. In addition, the intensity distribution over the vibronic bands changes with temperature: at 77 K an intense band is observable at 670  $\text{cm}^{-1}$ , and minor intensity, around 750  $\text{cm}^{-1}$  from the origin, while in the 1.2 K spectrum the band at 671  $\text{cm}^{-1}$  is weaker than the one at 749  $\text{cm}^{-1}$ . This might result from a temperature-induced population of states above the zero-point level of  $S_1$  and deserves further attention.

## Discussion

Our analysis of the vibronic structure of the fluorescence spectrum of molecular  $C_{60}$  indicates that appreciable vibronic coupling exists between the lowest excited singlet states with a concomitant mixed  $T_{1g}/G_g$  character of  $S_1$ . Previously magnetic-circular-dichroism<sup>3</sup> and fluorescence spectra<sup>6</sup> have been taken as evidence for the  $T_{1g}$  character of  $S_1$ . The fluorescence spectrum concerned the moderately resolved spectrum of  $C_{60}$  in a methylcyclohexane glass at 77 K (identical to the one in Figure 1b apart from a solvent-induced blue shift of about 40  $\text{cm}^{-1}$ ). The analysis of the vibronic intensity distribution in this spectrum on the basis of CNDO/S calculations led Negri et al.<sup>2</sup> to the  $T_{1g}$  assignment. Combining the results of these calculations with our highly resolved fluorescence spectra, measured for  $C_{60}$  in a decaline/cyclohexane glass (Figure 1c) and in a molecular crystal (Figure 3) at 1.2 K, leads to the

conclusion that the  $S_1$  state has not only  $T_{1g}$  character but also significant  $G_g$  and possibly minor  $T_{2g}$  character.

Besides modes active in the vibronic coupling between nondegenerate states, Jahn–Teller active modes show up in the fluorescence spectra as well. This particularly concerns  $h_g(1)$  and  $h_g(7)$ , which points to a distortion of  $C_{60}$  in the excited state along these coordinates. Negri et al. have calculated the expected Jahn–Teller distortion of  $C_{60}$  in several excited states<sup>1,2</sup> and concluded that the activity of  $h_g$  modes in the fluorescence from the  $T_{1g}$  state would be negligible. Our results indicate that the spectral activity of these modes might well be larger than suggested by the quantum-chemical calculations.

The interpretation of the fluorescence-excitation spectrum, summarized in Table 2, enables a description of the low-energy part of the absorption spectrum of  $C_{60}$ . The data in Table 2 directly provide for a description of the absorption spectrum in the 580–650 nm region of  $C_{60}$  in an argon matrix at 5 K reported previously.<sup>3</sup> The latter spectrum concerns a replica of the fluorescence-excitation spectrum in Figure 2 if we take into account a blue shift of about 230  $\text{cm}^{-1}$  upon going to the argon matrix. This positions the origin of the  $S_1 \leftarrow S_0$  transition in the argon matrix at 643 nm. Absorption spectra of  $C_{60}$  in the visible region in solution at room temperature have been reported by various authors, e.g. refs 4 and 11. We consider the absorption spectrum in *n*-hexane reported by Leach et al.<sup>4</sup> Although the spectrum is evidently much less resolved than the fluorescence-excitation spectrum at 1.2 K in Figure 2, the recognizable vibronic bands can be identified on the basis of

the data in Table 2 if we take into account a blue shift of about 50 cm<sup>-1</sup> upon going to *n*-hexane. The correspondence between the absorption and fluorescence-excitation spectrum is indicated in the last column of Table 2, where we have labeled the bands in the fluorescence-excitation spectrum with the band codes introduced by Leach et al. for the absorption spectrum. These authors have assigned the bands labeled  $\beta$  to triplet  $\leftarrow$  singlet vibronic transitions and those labeled  $\gamma$  to vibronic components of the first two singlet  $\leftarrow$  singlet transitions. Following our analysis of the fluorescence and fluorescence-excitation spectrum, we conclude that  $\beta_2$  more or less coincides with the electronic origin of S<sub>1</sub>  $\leftarrow$  S<sub>0</sub>, while the others correspond to vibronic components of this transition.

In the Introduction we mentioned that a vibrationally resolved spectrum of C<sub>60</sub> cooled in a supersonic molecular beam has been reported for the 595–635 nm region.<sup>5</sup> Sharp lines are visible at 622.0, 615.0, 609.5, 607.0, 605.2, 598.9, and 597.1 nm. The authors remark that the intense band at 607 nm may correspond to the 77 K solution absorption around 620 nm (i.e.  $\gamma_0$ ). This suggestion is supported by the analysis of absorption spectra of C<sub>60</sub> in a series of *n*-alkanes by Catalán,<sup>12</sup> which predicts  $\gamma_0$  at 607.3  $\pm$  0.2 nm for C<sub>60</sub> in the gas phase. From the fluorescence-excitation spectrum we know that  $\gamma_0$  is positioned 736 cm<sup>-1</sup> from the origin, which implies that the origin of the lowest excited state of gas phase C<sub>60</sub> should be at 635.4 nm. The bands observed by Haufler et al. then have the following energies relative to the origin: 339, 522, 669, 736, 785, 959, and 1010 cm<sup>-1</sup>. These vibrational quanta correspond well with those derived from the fluorescence-excitation spectrum of C<sub>60</sub> in decaline/cyclohexane and even better with those obtained from the 684-spectrum. Therefore, we propose for the seven bands observed in the supersonic beam an assignment similar to that of the corresponding bands in the latter 684-spectrum: vibronic bands of S<sub>1</sub>  $\leftarrow$  S<sub>0</sub> corresponding to h<sub>u</sub>(1), h<sub>u</sub>(2), t<sub>2u</sub>(2), h<sub>u</sub>(3), g<sub>u</sub>(2), g<sub>u</sub>(4), and h<sub>u</sub>(3) + h<sub>g</sub>(1) excitations, respectively.

Finally, we comment on a general observation that we made in our spectroscopic studies of C<sub>60</sub> and related species. All emission spectra that we obtained so far belong to one of two categories, characterized by a weak or by a relatively strong 0–0 transition. In Figure 4 we have plotted several spectra belonging to each of these categories on top of each other and shifted in such a way that their origins coincide. The left-hand side (Figure 4a) shows spectra with a weak origin: the fluorescence spectrum of a shallow molecular trap in crystalline C<sub>60</sub> at 1.2 K (the 684-spectrum), the fluorescence spectrum of C<sub>60</sub> in a decaline/cyclohexane glass at 1.2 K (the 658-spectrum), the corresponding fluorescence-excitation spectrum (on a reverse wavenumber scale), and the phosphorescence spectrum of C<sub>60</sub> in a decaline/cyclohexane glass at 1.2 K reported recently.<sup>13</sup> The right-hand side (Figure 4b) shows spectra with a strong origin. The top spectrum represents the fluorescence spectrum of deep X-traps in crystalline C<sub>60</sub> that consist of pairs of C<sub>60</sub> molecules.<sup>8</sup> The second spectrum concerns the fluorescence of C<sub>60</sub>O in decaline/cyclohexane at 1.2 K. A small amount of C<sub>60</sub>O was prepared by irradiating an oxygenated benzene/benzil (5:1 v/v) solution of C<sub>60</sub> with a mercury lamp, as described in ref 14. The reaction product was purified by HPLC, and mass spectrometry showed a purity of 98%. Its fluorescence spectrum shows a relatively strong origin at 680.9 nm and vibronic bands at 693.3, 704.6, 716.5, 731.1, 742.8, 755.4, 771.0, and 800.8 nm. The third spectrum in Figure 4b most probably represents

the fluorescence spectrum of a photoproduct of C<sub>60</sub>. In our laboratory we had an air-free solution of C<sub>60</sub> in decaline/cyclohexane ( $\sim 1.10 \cdot 10^{-4}$  M) whose fluorescence spectrum initially was identical to the 658-spectrum. After 2 weeks in modest daylight at room temperature, the emission spectrum at 1.2 K had converted into the spectrum in Figure 4b. This spectrum shows bands at 706.3, 719.6, 743.9, and 787.0 nm (with a precision of 0.5 nm); the band at 727.6 nm might well derive from unconverted C<sub>60</sub>. A similar spectrum was obtained upon illuminating an air-free solution of C<sub>60</sub> with 488 nm laser light (10 mW, spot diameter 3 mm) for several hours. The nature of the photoproduct has not been studied yet. The bottom spectrum in Figure 4b concerns the phosphorescence of C<sub>60</sub> that is induced by the presence of ethyl iodide in the solvent.<sup>13</sup> The correspondence between the spectra within each category is evident from panels a and b in Figure 4. We interpret this observation in the following way. For C<sub>60</sub> molecules in weak interaction with their surrounding (Figure 4a) the icosahedral symmetry of the molecule is decisive: the origin in the spectrum is weak, and the intensity is largely vibronically induced by Herzberg–Teller active modes. When the symmetry is lowered, the origin in the emission spectrum becomes strong and vibronic bands including totally symmetric and/or Jahn–Teller active modes show up (Figure 4b). The reduction in symmetry may result from intramolecular modification (C<sub>60</sub>O) or intermolecular interactions (C<sub>60</sub>/ethyl iodide) or from the delocalization of the excitation over a pair of C<sub>60</sub> molecules that has no inversion center.

**Acknowledgment.** The authors gratefully acknowledge A. C. J. Brouwer for his experimental contributions and M. A. Verheijen for growing the C<sub>60</sub> crystals. This work forms part of the research program of the “Stichting voor Fundamenteel Onderzoek der Materie” (FOM) and has been made possible by the financial support from the Netherlands Organization for Scientific Research (NWO).

## References and Notes

- (1) Negri, F.; Orlandi, G.; Zerbetto, F. *Chem. Phys. Lett.* **1988**, *144*, 31.
- (2) Negri, F.; Orlandi, G.; Zerbetto, F. *J. Chem. Phys.* **1992**, *97*, 6496.
- (3) Gasyna, Z.; Schatz, P. N.; Hare, J. P.; Dennis, T. J.; Kroto, H. W.; Taylor, R.; Walton, D. R. M. *Chem. Phys. Lett.* **1991**, *183*, 283.
- (4) Leach, S.; Vervloet, M.; Desprès, A.; Bréheret, E.; Hare, J. P.; Dennis, T. J.; Kroto, H. W.; Taylor, R.; Walton, D. R. M. *Chem. Phys.* **1992**, *160*, 451.
- (5) Haufler, R. E.; Chai, Y.; Chibante, L. P. F.; Fraelich, M. R.; Weisman, R. B.; Curl, R. F.; Smalley, R. E. *J. Chem. Phys.* **1991**, *95*, 2197.
- (6) Wang, Y. *J. Phys. Chem.* **1992**, *96*, 764.
- (7) Zeng, Y.; Biczok, L.; Linschitz, H. *J. Phys. Chem.* **1992**, *96*, 5237.
- (8) van den Heuvel, D. J.; Chan, I. Y.; Groenen, E. J. J.; Matsushita, M.; Schmidt, J.; Meijer, G. *Chem. Phys. Lett.* **1995**, *233*, 284.
- (9) Bethune, D. S.; Meijer, G.; Tang, W. C.; Rosen, H. J.; Golden, W. G.; Seki, H.; Brown, C. A.; de Vries, M. S. *Chem. Phys. Lett.* **1991**, *179*, 181.
- (10) Jishi, R. A.; Mirie, R. M.; Dresselhaus, M. S. *Phys. Rev. B* **1992**, *45*, 13685.
- (11) Aije, H.; Alvarez, M. M.; Anz, S. J.; Beck, R. D.; Diederich, F.; Fostiropoulos, K.; Huffman, D. R.; Krätschmer, W.; Rubin, Y.; Schriver, K. E.; Sensharma, D.; Whetten, R. L. *J. Phys. Chem.* **1990**, *94*, 8630.
- (12) Catalán, J. *Chem. Phys. Lett.* **1994**, *223*, 159.
- (13) van den Heuvel, D. J.; Chan, I. Y.; Groenen, E. J. J.; Schmidt, J.; Meijer, G. *Chem. Phys. Lett.* **1994**, *231*, 111.
- (14) Creegan, K. M.; Robbins, J. L.; Robbins, W. K.; Millar, J. M.; Sherwood, R. D.; Tindall, P. J.; Cox, D. M.; Smith, A. B., III; McCauley, J. P., Jr.; Jones, D. R.; Gallagher, R. T. *J. Am. Chem. Soc.* **1992**, *114*, 1103.

JP950643E